

Hot Water from Cold. The Dissociative Recombination of Water Cluster Ions<sup>†</sup>

R. D. Thomas,<sup>\*,‡</sup> V. Zhaunerchyk,<sup>‡,∇</sup> F. Hellberg,<sup>‡</sup> A. Ehlerding,<sup>‡</sup> W. D. Geppert,<sup>‡</sup> E. Bahati,<sup>§</sup> M. E. Bannister,<sup>§</sup> M. R. Fogle,<sup>§</sup> C. R. Vane,<sup>§</sup> A. Petrigani,<sup>||</sup> P. U. Andersson,<sup>⊥</sup> J. Öjekull,<sup>⊥</sup> J. B. C. Pettersson,<sup>⊥</sup> W. J. van der Zande,<sup>#</sup> and M. Larsson<sup>§</sup>

Department of Physics, Stockholm University, SE-106 91 Stockholm, Sweden, Physics Division, Oak Ridge National Laboratory, Oak Ridge, Tennessee 37831-6377, USA, FOM Instituut AMOLF, Kruislaan 407, 1098 SJ Amsterdam, The Netherlands, Department of Chemistry, Atmospheric Science, University of Gothenburg, SE-412 96 Gothenburg, Sweden, and Institute for Molecules and Materials, Radboud University Nijmegen, P.O. Box 9010, NL-6500 GL Nijmegen, The Netherlands

Received: October 7, 2009; Revised Manuscript Received: January 15, 2010

Dissociative recombination of the Zundel cation  $D_5O_2^+$  almost exclusively produces  $D + 2 D_2O$  with a maximum kinetic energy release of 5.1 eV. An imaging technique is used to investigate the distribution of the available reaction energy among these products. Analysis shows that as much as 4 eV can be stored internally by the molecular fragments, with a preference for producing highly excited molecular fragments, and that the deuteron shows a nonrandom distribution of kinetic energies. A possible mechanism and the implications for these observations are addressed.

## Introduction

Gas-phase molecular clusters represent a way of studying phenomena of interest in bulk but with the precision of gas-phase methods. Water cluster ions, that is,  $H^+(H_2O)_n$ , are one of the most important examples of such species, as  $n$  increases they span the range between gas and condensed phase systems. The high mobility and structure of the hydrated proton in water have long puzzled researchers. The large proton affinity of  $H_2O$  means the proton cannot exist in isolation, and the smallest water clusters vary between proton-bridge structures, for example, the “Zundel” cation ( $H^+(H_2O)_2$ ,  $n = 2$ ), and oxonium ion ( $H_3O^+$ ,  $n = 1$ ) centered, for example, the “Eigen” cation ( $H_3O^+(H_2O)_3$ ,  $n = 4$ ). Liquid-phase experiments show the transition time scale between the Zundel and Eigen forms is fast, with proton transfer occurring in less than 100 fs, and that the delocalized proton’s zero-point energy is important; for example, in the Zundel cation the proton essentially rattles around in-between the two oxygen atoms without any effective potential barrier,<sup>1,2,4–8</sup> highlighting the complicated nature of these systems.<sup>1–3</sup> Proton motion is then significant in any dynamics<sup>4,6–8</sup> and the Zundel cation represents the ideal system for investigating these dynamics.

Water cluster ions occur naturally in the D region of the earth’s atmosphere (60–90 km)<sup>9</sup> and nominally reach a cluster size of  $n = 6$  though in the cold polar regions clusters up to  $n = 21$  have been observed.<sup>10</sup> In the top few kilometers of the D region the electron density decreases by almost an order of magnitude. The dominant mechanism behind this decrease is dissociative recombination (DR).<sup>11</sup> In DR, a molecular ion recombines with a free electron and dissociates into neutral products (see e.g., refs 12–13). DR with water cluster ions

would terminate clustering, preventing further growth.<sup>14</sup> Indeed, the DR of  $n = 2–6$  clusters efficiently leads to the predominant (>80%) production of  $nH_2O + H$ .<sup>3,15,16</sup> Extensive mid-infrared lasing by water molecules has been reported in a supersonic plasma expansion where it was suggested that the necessary population inversion could be produced through the DR of water cluster ions<sup>17</sup> since DR is known to lead to population inversions and strong mid-IR to far-IR laser action in H atoms.<sup>18</sup> The DR of the fully deuterated Zundel cation, chosen for experimental reasons,<sup>3,12</sup> produces almost exclusively (>95%) two  $D_2O$  molecules and a D atom, with a maximum kinetic energy release of 5.1 eV. By revealing the dynamics occurring in this reaction we report here on the distribution of the available energy in this channel and furthermore suggest a mechanism capable of explaining the observation of the lasing lines in a water plasma as well as shine light on the elusive nature of the solvated proton.

## Experimental Section

Studies at ion storage rings on the DR of  $XH_2^+$  type ions, where X is a heavy atom, for example C, covalently bonded to two H atoms, show that the H atoms are extremely mobile;  $X + H_2$  is often observed to be populated at 10% of the reaction flux.<sup>12,13</sup> Several such ions have a linear ionic ground-state geometry, indicating that extreme bending or tunnelling must be occurring during the reaction to explain the observation of this channel. Importantly, similar motion in heavier systems, for example,  $CO_2^+$  to form  $C–O_2$ , has never been observed<sup>12</sup> pointing to the mobile and quantum nature of the H atom. Extreme motion is also observed in the dominant product channel of these ions ( $X + 2H$ )<sup>12,19</sup> and so investigating the dynamics in the dominant channel in the DR of the Zundel cation should prove enlightening.

Investigating the internal energy of molecular fragments in the DR process is difficult and nontrivial from experimental and theoretical perspectives. Experimental studies into the DR of  $H_3^+$ ,  $H_3O^+$  and  $CH_5^+$  have shown that vibrationally excited fragments are produced.<sup>21,26,27</sup> A theoretical treatment of the DR of  $NH_4^+$  has been reported, both supporting the experimental

<sup>†</sup> Part of the special section “30th Free Radical Symposium”.

<sup>\*</sup> To whom correspondence should be addressed. E-mail: rdt@fysik.su.se.

<sup>‡</sup> Stockholm University.

<sup>§</sup> Oak Ridge National Laboratory.

<sup>||</sup> FOM Instituut AMOLF.

<sup>⊥</sup> University of Gothenburg.

<sup>#</sup> Radboud University.

<sup>∇</sup> Current Address: Institute for Molecules and Materials, Radboud University Nijmegen.

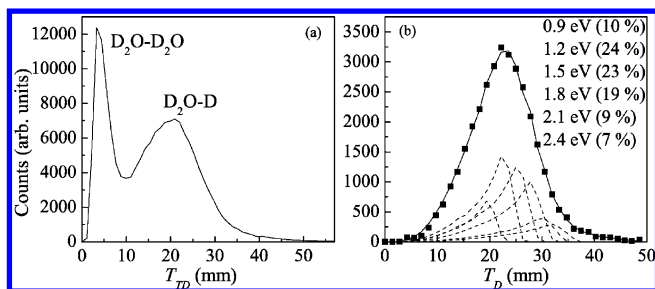


**Figure 1.** (a) Experimentally measured  $T_{TD}$  distribution. (b)  $T_D$  distributions for experimental data (solid squares) and data sets generated from a Monte Carlo simulation which have a contribution larger than 2% are shown by dashed curves. The quoted energy corresponds to the kinetic energy given to the fragments in these contributing data sets. The best-fit is shown by the solid curve.

result that  $\text{NH}_3 + \text{H}$  is the dominant channel and predicting the reaction-energy partitioning among the products; the dominant share of the available energy (4.7 eV) is given to vibrational excitation of the  $\text{NH}_3$  fragment with an average value of  $E_v = 4.0 \pm 0.2$  eV, and little to rotation or translation.<sup>28</sup> However, for  $\text{H}_3^+$  the channel  $\text{H}_2 + \text{H}$  does not dominate in zero eV collisions and for the other ions the amount of energy available for internal excitation of the molecular product in the dominant channel is low since multiple covalent bonds are broken. It is certainly not clear or predictable how the available energy would be distributed in a cluster ion, in which the structure is determined by the weakest bonds and the dominant channel involves breaking two such bonds while still leaving over 5 eV of energy available for use.

The current experiment has been performed at CRYRING, Stockholm University, and the facility and experimental procedures are described in detail elsewhere and are not discussed here.<sup>12</sup> The data were obtained with an imaging detector which measured only the positions of the neutral products produced in the reaction, so-called 2D data.<sup>12,13</sup>

## Results and Analysis

Defining the total displacement,  $T_D$ , as

$$T_D = \left( d_D^2 + \frac{m_2}{m_1} (d_{(\text{D}_2\text{O})_1}^2 + d_{(\text{D}_2\text{O})_2}^2) \right)^{0.5} \quad (1)$$

where  $m_1$  and  $m_2$  are the D and  $\text{D}_2\text{O}$  masses, respectively, and  $d_x$  is the distance of fragment  $x$  from the center-of-mass (com), the kinetic energy available to the fragments can be found, that is, small  $T_D$  means less kinetic energy is released and higher internal excitation of the water molecules. To establish a com position the fragments must be identified, and since this is not explicitly possible the following approach is employed. The three fragments define the break-up triangle and the length of each side is histogrammed,  $T_{TD}$ . The  $T_{TD}$  distribution for all accepted events is plotted in Figure 1(a). Analysis of this distribution shows two peaks; one at very small and one at very large distances, and these are expected to correspond to the  $\text{D}_2\text{O}-\text{D}_2\text{O}$  and  $\text{D}-\text{D}_2\text{O}$  intrafragment separations, respectively. Based on this, the fragments were assigned in the following way: the fragment which is further away from the other two than they are from each other should be D atom. Indeed, if the fragments receive the same momenta upon break-up, the displacement of the D will be 10 times larger than those of the  $\text{D}_2\text{O}$  fragments. Having defined the com, the solid squares in Figure 1b show the experimentally determined  $T_D$  distribution.

Although this assignment procedure generally is not valid, for example, it is incorrect for linear or close-to-linear  $\text{D}_2\text{O}-\text{D}-\text{D}_2\text{O}$  geometries, we motivate its validity in the present case by demonstrating from analysis of the break-up dynamics that such geometries are not important in this reaction. One method often used to visualize break-up dynamics is the Dalitz plot.<sup>12,20-22</sup> The coordinates of the Dalitz plot are defined as

$$\eta_1 = \frac{1}{3} \sqrt{\frac{m_3}{m_1}} (c - b) \quad (2a)$$

$$\eta_2 = \frac{1}{3} \left[ \left( 2 + \frac{m_1}{m_2} \right) a - 1 \right] \quad (2b)$$

where  $m_3$  is the  $\text{D}_5\text{O}_2$  mass, and  $a$ ,  $b$ , and  $c$  are the fraction of the available kinetic energy,  $E_a$ , received by the D and two  $\text{D}_2\text{O}$  molecules, respectively, such that  $a + b + c = 1$ . To help with the analysis, if we define  $b < c$ , then conservation of kinetic energy and momentum dictate that  $a$  and  $b$  are given by:

$$0 \leq a \leq \frac{2m_2}{m_3}$$

$$\frac{1}{2} \left[ (1 - a) - \frac{\sqrt{am_1(2m_2 - am_3)}}{m_2} \right] \leq b \leq \frac{1}{2}(1 - a) \quad (3)$$

Each point on the Dalitz plot corresponds to a particular dissociation geometry, illustrated in Figure 2a.

The experimental data are the transverse projections of the fragment's com momenta randomly oriented in space with respect to the detector plane, so to extract the actual dissociation geometries a Monte Carlo (MC) simulation is used to account for all possible orientations of the molecular frame as well as other experimental considerations, that is, it allows us to model the response of our detector.<sup>22,21,22</sup> This approach was first used by Müller and Cosby to investigate dynamics in the fragmentation of  $\text{H}_3^+$ <sup>23</sup> and subsequently has also proven valuable in DR.<sup>12,19</sup> The deconvolution procedure described in refs 21 and 24 implies that the experimentally measured Dalitz plot must be divided by that generated by the MC simulation in which the break-up molecular geometries were fully randomized. Those geometries which would be mischaracterised due to the assignment procedure are shown by the blank regions in Figure 2b. Figure 2c shows simulated data in which the break-up geometry is completely randomized. Figure 2d plots the ratio of the experimental data shown in 2b to the simulated data shown in Figure 2c and so reflects the real fragmentation dynamics. Analysis indicates that the fragmentation is not random but that the distribution of deuteron kinetic energies shows definite structure.

Information about the break-up dynamics can also be obtained from the distributions of the parameters  $a$  and  $b$ , which are independently retrieved in a fashion similar to that utilized for the Dalitz plot. Figure 3a plots the experimental data while Figure 3b shows simulated data where one of the investigated parameters, either  $a$  or  $b$ , was fully randomized. Normalizing the experimental data set to the simulated random data set gives the true distributions and these are shown in Figure 3c. The kinetic energy of the D atom is not random, showing a broad peak with a maximum at  $a \approx 0.8$ . These results are consistent

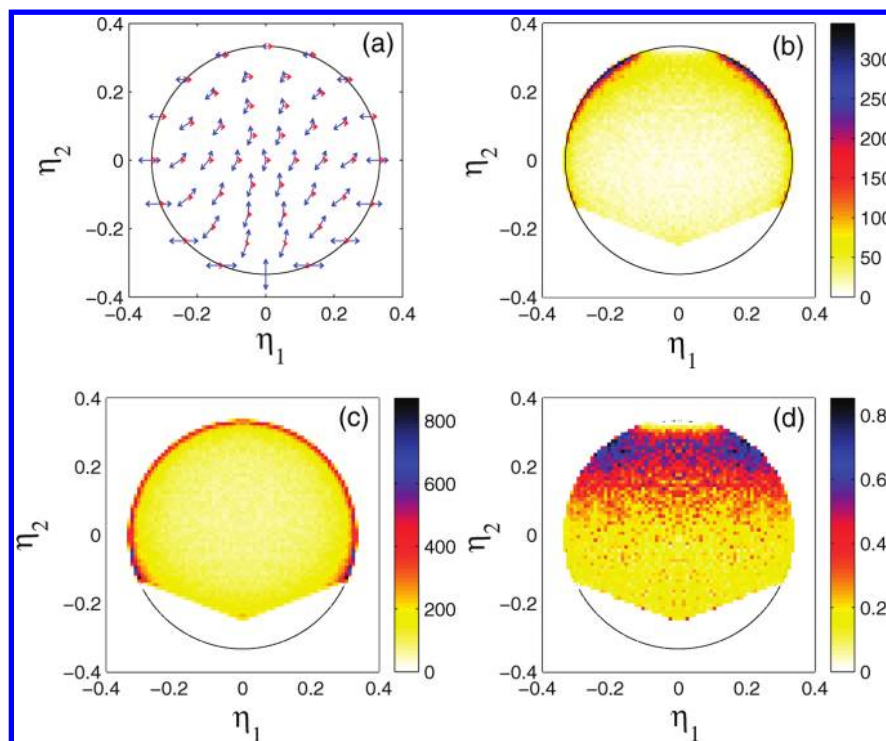


**Figure 2.** Dalitz plots showing: (a) The break-up geometries constructed from the fragment momentum vectors. The momentum of the D atom is shown in red. (b) The experimental data. (c) The results from the Monte Carlo simulation assuming a random distribution of break-up geometries in the molecular frame. (d) The real distribution of geometries.

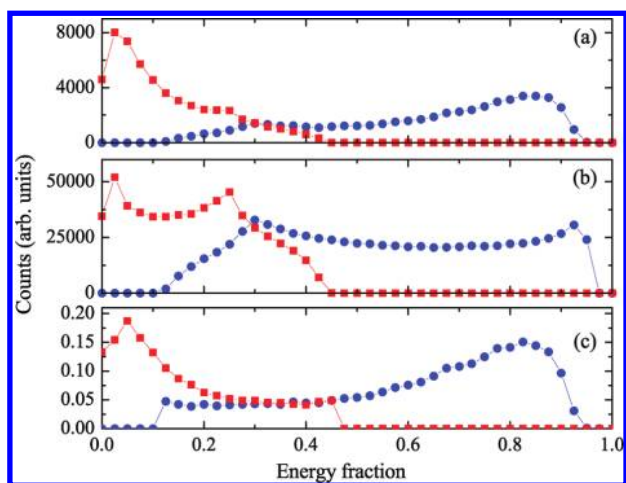


**Figure 3.** The parameters  $a$  and  $b$  represent the energy sharing between the three fragments. The top plot (a) shows the experimental data, the middle plot (b) shows data from the Monte Carlo simulation for which all allowed values of one of the investigated parameters,  $a$  or  $b$ , are equally probable. The bottom plot (c) shows the result obtained when the experimental data (a) is normalized by the simulated data (b). In each plot  $a$  and  $b$  are shown as solid circles and squares, respectively.

with the derived distributions in the Dalitz plot. According to eq 2a, the range of  $a$  values from 0.75 to 0.9 will correspond to  $\eta_2$  values ranging from 0.19 to 0.3. Furthermore, if additionally we consider distribution of parameter  $b$  in the range of 0.025–0.075 with  $a$  being 0.8, the corresponding  $\eta_1$  values are from 0.08 to 0.23.

It is instructive to verify the validity of the fragment assignment procedure. The derived  $a$  and  $b$  distributions were used as input parameters for the simulation that generated break-up triangles defined by the three fragments, and the following sets of parameters, which are independent of particle assignment,

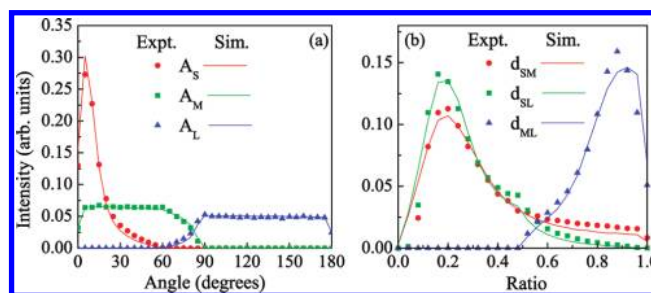


**Figure 4.** Three internal angles (a) and three distance ratios (b) of the break-up triangle. Experimental data are given by the solid symbols and the solid lines show the results from the Monte Carlo simulation.

were extracted: the ratio of the sides in the break-up triangle; shortest/medium ( $d_{SM}$ ), shortest/longest ( $d_{SL}$ ), and medium/longest ( $d_{ML}$ ), and the three internal angles of this triangle; largest ( $A_L$ ), medium ( $A_M$ ), smallest ( $A_S$ ). When these parameters are generated using random distributions of  $a$  or  $b$  the results do not fit the experimental observations whereas those obtained using the normalized distributions shown in Figure 3(c) fit extremely well, and these results are shown (solid lines) in Figure 4 together with the experimentally determined distributions (solid symbols). The method of particle assignment will always be wrong for linear or close-to-linear  $D_2O-D-D_2O$  geometries. However, the lack of a peak at large internal angles (Figure 4a) allowed us to conclude that the molecule hardly ever dissociates from such geometries. As such, the particle assignment procedure used in calculating  $T_D$  is reliable for almost all of the events analyzed. Since  $T_D^2$  is directly proportional to  $E_{av}$ , distribution of the available reaction energy can now be investigated by analysis of the  $T_D$  data without biasing the results. It is important to point out that the Dalitz plot is probably more accurate when obtaining dynamical information, since it shows the correlation between the  $a$  and  $b$

parameters. However, the main reason to retrieve the  $a$  and  $b$  parameters independently was to use them in the Monte Carlo simulation to check the validity of the assignment procedure and to obtain the  $T_D$  distributions.

Due to the experimental conditions and the small difference between ro-vibrational energy levels,  $T_D$  distributions are generated by the simulation for values of  $E_\alpha$  from 0 to 5.1 eV in steps of 0.3 eV. The individual distributions are then scaled and the sum is compared with the experimental data. The relative contribution of each channel to the best-fit summed distribution can then be extracted. The results are shown in Figure 1b, where the dashed lines plot individual distributions, the solid line are the best-fit sum, and the relative contribution of each channel is also given. Analysis shows that as much as 4 eV is partitioned into internal excitation of the water molecules and that low excited states are not significantly populated.

## Discussion

In the Zundel cation the proton oscillates back and forth between the two water molecules over an almost barrier-less potential surface.<sup>4–8</sup> In direct DR, the neutral system is created directly on a repulsive surface which promptly dissociates.<sup>12,13</sup> Here, this will map each D<sub>2</sub>O with their Zundel ion-geometry onto the ground state D<sub>2</sub>O surface. However, since the differences in the bond-lengths and internal angles between these two states are significantly less than 10%,<sup>5</sup> this mechanism would induce very little excitation in the fragments and so is unlikely to be the relevant mechanism here. In indirect DR, the electron excites nuclear motion and is captured into a vibrationally excited Rydberg state.<sup>12,13</sup> For a Rydberg state with D<sub>5</sub>O<sub>2</sub><sup>+</sup> as the ion core, if it is the proton's motion which is vibrationally excited, the weak potential surface would allow the proton to undergo multiple high-energy collisions with the water molecules before the system dissociates. Leone and co-workers reported that translational-to-vibrational energy transfer in collisions of 2.2 eV H atoms with H<sub>2</sub>O molecules was extremely effective, and multiple emitting states with high vibrational and rotation quantum numbers were observed to be created in these collisions.<sup>25</sup> Here, this would create the highly rovibrationally excited water molecules which are observed experimentally. Since these states are created in a similar collision mechanism to that investigated by Leone and co-workers, the subsequent decay of these states could also be responsible for the lasing observed in the experiments of Saykally and co-workers and confirm DR as the responsible reaction mechanism.<sup>17,25</sup> It cannot be ruled out that the deuteron leaves without interacting and excites other water molecules. However, (Figure 3c) the fraction of the kinetic energy taken by the deuteron is very broad and although it peaks at  $\approx 0.85$ , the actual kinetic energy available to the fragments (Figure 1b) is predominantly less than 1.8 eV, implying that the majority of deuterons are produced with kinetic energies much less than 1.5 eV, and the efficiency of impulse-excitation is predicted to be sensitive to the translational energy.<sup>25</sup>

These investigations show that the formation of vibrationally excited products should be the first thought when considering DR reactions and not the last, and that the formation of nonstatistical and highly excited vibrational populations are likely.

## Conclusion

Excited water molecules are efficiently produced in the DR of the Zundel cation and, furthermore, are created with a nonthermal vibrational population. We conclude that only the indirect DR process through excitation of the proton motion is capable of creating the states necessary to produce the rovibrationally excited water molecules, in a collisional process similar to that observed by Leone and co-workers,<sup>25</sup> and that the subsequent decay of these states could also explain the observed mid-infrared lasing reported in a supersonic plasma expansion.<sup>17</sup> Although it cannot be ruled out that the deuterons produced in the reaction excite other water molecules in the plasma, analysis shows that they would have a broad range of kinetic energies much less than 1.8 eV and, since it is predicted that the efficiency of the excitation is sensitive to the translational energy,<sup>25</sup> it is not clear that this would be sufficient to explain the observed lasing and so plasma modeling is necessary to determine the effectiveness of this process. In either case, DR would be the initial reaction mechanism responsible for the observed lasing.

**Acknowledgment.** The authors thank the CRYRING staff at the Manne Siegbahn Laboratory for their tireless work and excellent support. This work was supported by the Swedish Research Council and STINT. RDT is funded under the IHP Programme of the EC under contract HPRN-CT-2000-00142. The work of WJvdZ is part of the research of the “Stichting voor Fundamenteel Onderzoek der Materie”. EB, MEB, MRF, and CRV are supported by the U.S. DOE, Office of Basic Energy Sciences under contract DE-AC05-00OR22725 with UT-Battelle, LLC.

## References and Notes

- (1) Hynes, J. T. *Nature* **1999**, *397*, 565.
- (2) Marx, D.; et al. *Nature* **1999**, *397*, 601–604.
- (3) Någård, M. B.; et al. *J. Chem. Phys.* **2002**, *117*, 5264–5270.
- (4) Woutersen, S. *Phys. Rev. Lett.* **1999**, *402*, 507.
- (5) Ojamäe, L. *J. Chem. Phys.* **1998**, *109*, 5547.
- (6) Woutersen, S.; Bakker, H. J. *Nature* **2006**, *96*, 138305.
- (7) Xantheas, S. S. *Nature* **2009**, *457*, 673.
- (8) Vendrell, O. *Angew. Chem., Int. Ed.* **2009**, *48*, 352–355.
- (9) Brasseur, G.; Solomon, S. *Aeronomy of the Middle Atmosphere*; Reidel: Dordrecht, 1986.
- (10) Björn, L.; Arnold, F. *Geophysics Research Letters* **1981**, *8*, 1167.
- (11) Wayne, R. P. *Chemistry of Atmospheres*, Third ed.; Oxford Science Publications: Oxford, 2000.
- (12) Thomas, R. D. *Mass Spectrom. Rev.* **2008**, *27*, 485.
- (13) Larsson, M.; Orel, A. *Dissociative Recombination of Molecular Ions*; Cambridge University Press: Cambridge, 2008.
- (14) Rapp, M. J. *Atmos. Solar-Terr. Phys.* **2001**, *63*, 759.
- (15) Öjekull, J.; et al. *J. Chem. Phys.* **2007**, *125*, 194301.
- (16) Öjekull, J. *J. Chem. Phys.* **2008**, *128*, 044311.
- (17) Micheal, E. A. *Chem. Phys. Lett.* **2001**, *338*, 277.
- (18) Thum, C.; et al. *Astron. Astrophys.* **1998**, *333*, L63.
- (19) Larsson, M.; Thomas, R. *Phys. Chem. Chem. Phys.* **2001**, *3*, 4471.
- (20) Dalitz, R. H. *Philosophy Magazine* **1953**, *44*, 1068.
- (21) Strasser, D.; et al. *Phys. Rev. Lett.* **2001**, *86*, 779.
- (22) Zhaunerchyk, V.; et al. *Phys. Rev. Lett.* **2007**, *98*, 223201.
- (23) Müller, U.; Cosby, P. C. *Phys. Rev. A* **1999**, *59*, 3632.
- (24) Thomas, R.; et al. *Phys. Rev. A* **2002**, *66*, 032715.
- (25) Lovejoy, C.; et al. *J. Chem. Phys.* **1992**, *96*, 7180.
- (26) Zhaunerchyk, V.; et al. *J. Chem. Phys.* **2009**, *130*, 214302.
- (27) Zhaunerchyk, V.; et al. *Phys. Rev. Lett.* **2009**, *98*, 090701(R).
- (28) Öjekull, J.; et al. *J. Chem. Phys.* **2004**, *120*, 7391.